Reduction of Silver Oxide Film in Inert Gas Plasma

Victor Ovchinnikov
Department of Aalto Nanofab
School of Electrical Engineering, Aalto University
Espoo, Finland
e-mail: Victor.Ovchinnikov@aalto.fi

***Abstract*— Reduction of silver oxide in plasma is studied. Silver oxide film was prepared by plasma oxidation of thermally evaporated silver film. It is shown that silver oxide is reduced with different rate in He, Ar and N_2 plasmas excited by rf power. To clarify mechanism of reduction, morphology, electrical and optical properties of the samples are analyzed. Spectroscopic ellipsometry is used to measure thicknesses and optical constants of oxidized and reduced layers. It is concluded that the reduction is activated by low energy electron bombardment of silver oxide.**

Keywords-silver oxide; plasma reduction; silver thin film.

I. INTRODUCTION

Both silver and silver oxide are widely used as functional material in microdevices. Silver is the best plasmonic material in visible range and has found broad application in sensors, photonics, catalysis and spectroscopy [1]. Unique properties of silver oxide are used in optical storage devices, gas sensors, photovoltaic cells and photonics [2]. Silver and silver oxide are applied both in the form of thin films, and in the form of nanostructures. Additionally, non-stoichiometric silver oxide Ag_xO or silver oxide with silver inclusions can be used instead of pure oxide. Properties of silver oxide nanostructures and thin films are found to be sensitive to fabrication method. It has caused a big variety of the applied methods, such as thermal evaporation [3], reactive magnetron sputtering [4], chemical-bath deposition [5], exposing silver films to atomic oxygen environment [6][7], and so on. The last method is very attractive, because it opens an opportunity for application of well known Ag deposition methods in preparation of silver oxide films. Furthermore, interconversion of Ag into Ag_xO and Ag_xO in Ag would be desirable for fabrication of silver containing nanostructures and Ag_xO films with controlled silver content. Suitable reduction process of Ag_2O to Ag would be also benefit for removing of native oxide layer from silver structures (SERS substrates etc.) after long storage. However, reports about reciprocal conversion of Ag_xO into Ag in dry ambient (gas, plasma) are concentrated on application of reducing agents like H_2 or annealing in inert ambient [8][9]. In the first case, the reducing agent can involve undesirable reactions with other materials of microdevice. In the second case, high temperature can limit choice of materials used in fabrication process. Nevertheless, publications about conversion of Ag_xO into Ag without reducing agents are occasional and devoted to interaction of Ag_xO surface with energetic particles.

In this paper, we propose to use inert gas plasma for dry reduction of silver oxide films. It is demonstrated that conversion of Ag_xO in Ag is possible in a standard reactor for dry etching using Ar, He or N_2 plasma. The reduction rate is proportional to ionization degree of plasma, i.e., concentration of electrons near processed sample. Ag content in the obtained films depends on plasma gas and can be controlled in broad range by process parameters, including reduction time, pressure and rf power.

The paper is organized in a following way. In the subsequent Section II, details of sample preparation and measurement procedures are presented. In Section III, results of the work are demonstrated by scanning electron microscope (SEM) images, electrical measurements as well as ψ, Δ spectra and reflection spectra of the fabricated samples. In Section IV, possible reduction mechanism of Ag_2O in inert gas plasma is discussed. In Section V, the conclusion is drawn.

II. EXPERIMENTAL DETAILS

A crystalline Si wafer (100 mm in diameter, 0.5-mm-thick, <100>) was used as a substrate. To increase accuracy of optical measurements, a 609 nm thick SiO_2 layer was prepared by thermal oxidation of the Si wafer. A 15 nm thick silver layer was deposited by electron-beam evaporation with the deposition rate of 0.3 nm/s and base pressure 2×10^{-7} Torr. All plasma treatments were made in two identical parallel plate reactors, which differ by sample position in a reactor. In the plasma etching (PE) reactor the sample was fixed on grounded electrode, in the reactive ion etching (RIE) reactor the sample was fixed on isolated electrode. Metal deposition and plasma treatments were done at room temperature.

Plasma oxidation was done in PE reactor during 90 seconds at oxygen flow of 100 sccm, pressure 1000 mTorr and rf power 20W. Several identical Ag_xO samples were prepared to compare reduction in different conditions. For this purpose the whole wafer was cut on chips (2×2 cm^2), which were further processed separately, but at the same pressure 500 mTor and during the same time 60 s. The sample #1 was treated in RIE reactor at Ar flow 50 sccm, the samples #2, #3 were processed in PE reactor at flow 500 sccm of He and N_2, respectively. Diluted ammonia solution (NH_3 25 % from Honeywell) NH_3:H_2O = 1:1 was used for selective etching of Ag_2O. This treatment does not affect on Ag, Si and SiO_2. All samples were etched during 20 s.

 ISBN: 978-1-61208-495-4

Silver film was deposited in e-beam evaporation system IM-9912 (Instrumentti Mattila Oy, Finland). Plasma treatments were done in 13.56 MHz driven parallel electrode reactors Plasmalab 80 Plus (Oxford Instruments Plasma Technology). To investigate the prepared samples, plane-view image observations were performed in Zeiss Supra 40 field emission scanning electron microscope. Spectroscopic ellipsometry (SE) measurements in the range of 700–1700 nm at the angle 70º were done by spectroscopic ellipsometer SE 805 (SENTECH Instruments GmbH). Sheet resistance of films was measured by four points probe method. Reflectance measurements were carried out using a FilmTek 4000 (Scientific Computing International, USA) reflectometer at normal light incidence in the spectral range 400–1700 nm.

III. RESULTS

In this section, the results of sequential oxidation of as deposited silver film and reduction of obtained silver oxide film are reported. To justify silver oxidation and Ag_xO reduction, comparison of electrical, optical and chemical properties is performed.

A. Oxidation

In the beginning, reflection measurements for as deposited and plasma-oxidized silver films were made. Due to thick SiO_2 layer (609 nm), reflection from the Si substrate and low absorption in the upper layer, interference effects have been observed in both films (Fig. 1). It was noted that interference maxima of the silver film at 570 nm and 830 nm correspond to interference minima of the Ag_xO film at the same wavelengths. Taking into account negligible optical thickness of the upper layer (less than $\lambda/8$) and identical thicknesses of SiO_2 layers, this fact can be only explained by different phase shift upon reflection from Ag and Ag_xO layers. Difference in phase shift is close to 180°. It means that the original metal layer has been converted into dielectric one after oxidation [10]. The formation of silver oxide is also evident from wet etching in ammonia solution. Silver film remains invariable, but A_xO film is totally removed. The SEM images also confirm difference between as deposited and oxidized silver

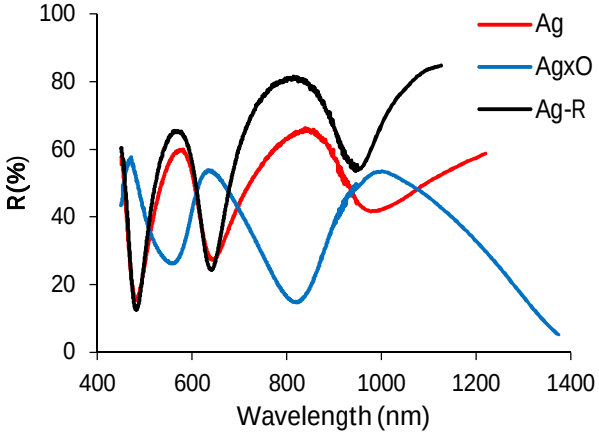

Figure 1. Reflection spectra of as deposited, oxidized and reduced (sample #2) Ag films.

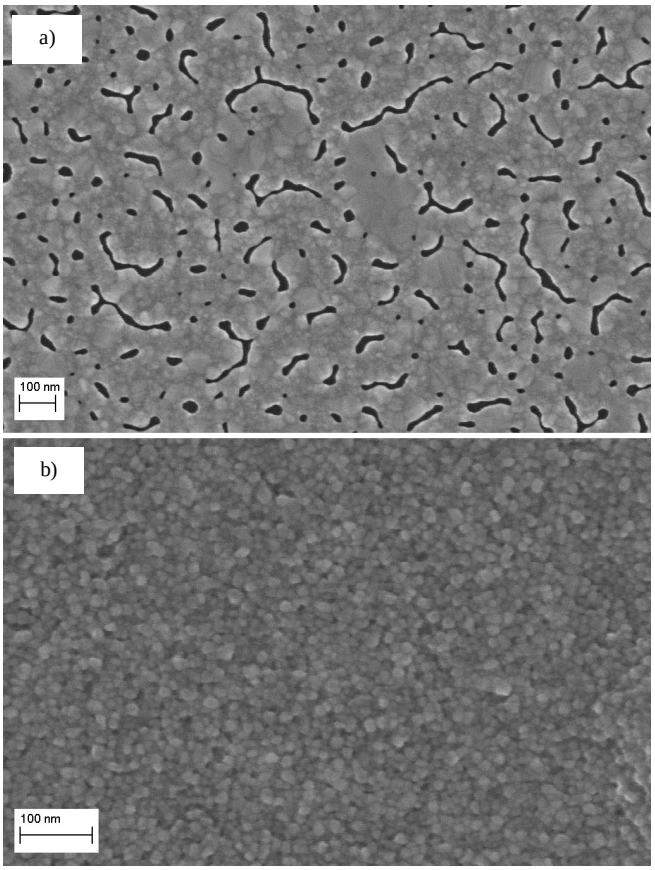

Figure 2. SEM images of as deposited (a) and oxidized (b) Ag films.

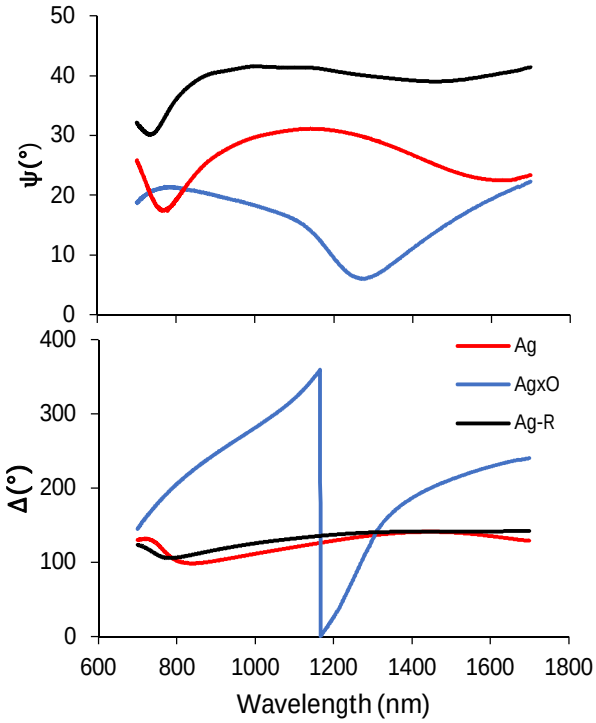

Figure 3. ψ, Δ spectra of as deposited, oxidized and reduced (sample #1) Ag films.

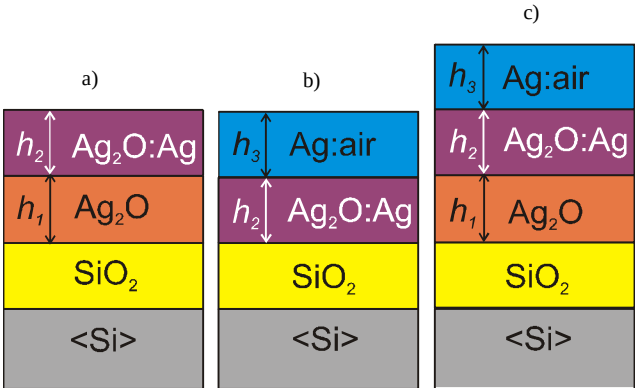

Figure 4. Optical models of Ag_xO (a), Ag reduced in He or Ar (b), Ag reduced in N_2 (c).

films (Fig. 2). The discontinuous Ag film, including voids of random shape converts in agglomeration of closely packed crystallites. Cubic shape of crystallites resembles cubic crystalline structure of Ag_2O.

To measure optical constants of oxidized silver, SE was used. It is based on measurement of ellipsometric angles ψ, Δ in the range of wavelengths. After that the sample is described by simplified model from several optical layers and ψ, Δ are calculated for the model. Then, matching between measured and calculated ψ, Δ is done for different parameters of optical layers. The obtained ψ, Δ spectra of as deposited and oxidized silver films are given in Fig. 3. Totally different ψ, Δ curves before and after oxidation confirm conversion of Ag into Ag_xO.

To extract optical constants of the oxidized silver, the ellipsometric spectra were analyzed by model with layered structure. The model contains the pure Ag_2O layer (thickness h_1) and the Ag_2O:Ag layer (thickness h_2), as shown in Fig.4a. The A_2O:Ag composite was described in the assumption that it consists of Ag_2O matrix and Ag inclusions. The dielectric function of composite was calculated according to the Bruggemann effective-medium approximation (EMA). The unknown dielectric function of the Ag_2O was found by using Tauc-Lorentz dispersion formula with two oscillators. Parameters of these Lorentz oscillators are linked to imaginary part of the dielectric function and are listed in Table I. A_i is related to strength of the i-th absorption peak (i=1,2), C_i is the damping coefficient of the i-th oscillator, E_i is the energy position of the i-th peak. Two additional parameters are optical band gap energy E_g = 0.21 eV and high frequency dielectric constant ε_∞ = 1.06.

TABLE I. PARAMETERS OF Ag_2O MODEL

Oscillator no.	A (eV)	E (eV)	C (eV)
1	7,30	4,27	0,15
2	20,80	3,20	2,40

The obtained model parameters for Ag_xO are given in Table II. Silver fraction in the composite layer A_2O:Ag is 0.07 and total thickness of the layer (h_1+h_2) has increased to 34.5 nm after oxidation. The wavelength dependences of the extracted refractive index n and extinction coefficient k for Ag_2O are shown in Fig. 5. Both of them are higher than

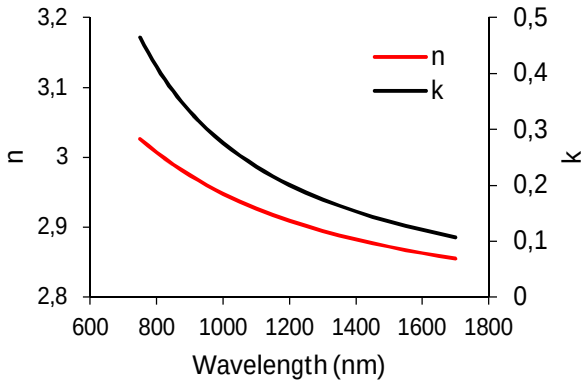

Figure 5. Optical constants of Ag_xO.

reported values for sputtered Ag_2O [4]. Both of them follow normal dispersion, i.e., decrease for longer wavelength in contrast to silver optical constants, which increase with wavelength. The purpose of optical calculations is justification of oxidation or reduction reactions in plasma ambient. In this context, absolute values of optical constants are not so significant as their variations in response on process parameter changing.

B. *Reduction*

The wafer with silver oxide was cut in chips for reduction experiments in different conditions. In Fig. 1, reflection

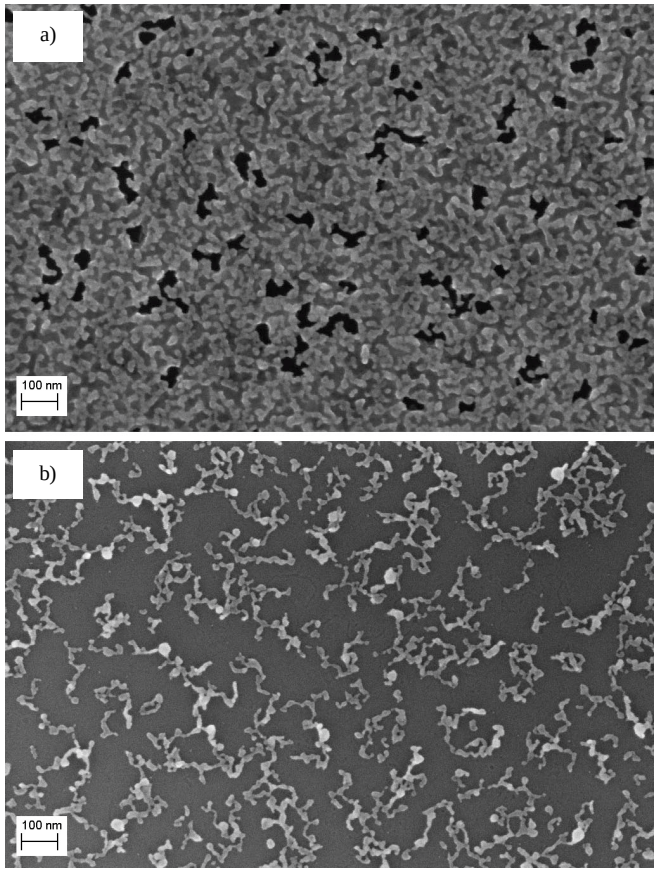

Figure 6. SEM images of the sample #3 after reduction (a) and after NH_3 etching (b).

TABLE II. SAMPLE PREPARATION PARAMETERS AND MEASUREMENT RESULTS

Sample	Reactor	Gas	Power, W	ρ, Ω m	Ag_2O	Ag_2O:Ag		Ag:air		Total	
					nm	*nm*	*Ag*[a]	*nm*	*air*[b]	*Thickness, nm*	*Ag*[a]
Ag				$7{,}1\times10^{-8}$						15,0	
Ag_2O	PE	O_2	35	$6{,}4\times10^{-1}$	18,0	16,5	0,07			34,5	0,03
#1	RIE	Ar	12	$8{,}0\times10^{-8}$		6,9	0,84	14,3	0,05	21,2	0,91
#2	PE	He	20	$9{,}7\times10^{-8}$		12,5	0,82	8,8	0,18	21,2	0,82
#3	PE	N_2	20	$1{,}3\times10^{-6}$	6,0	6,9	0,30	10,2	0,44	23,1	0,34

a. Ag fraction in the layer.

b. Air fraction in the layer.

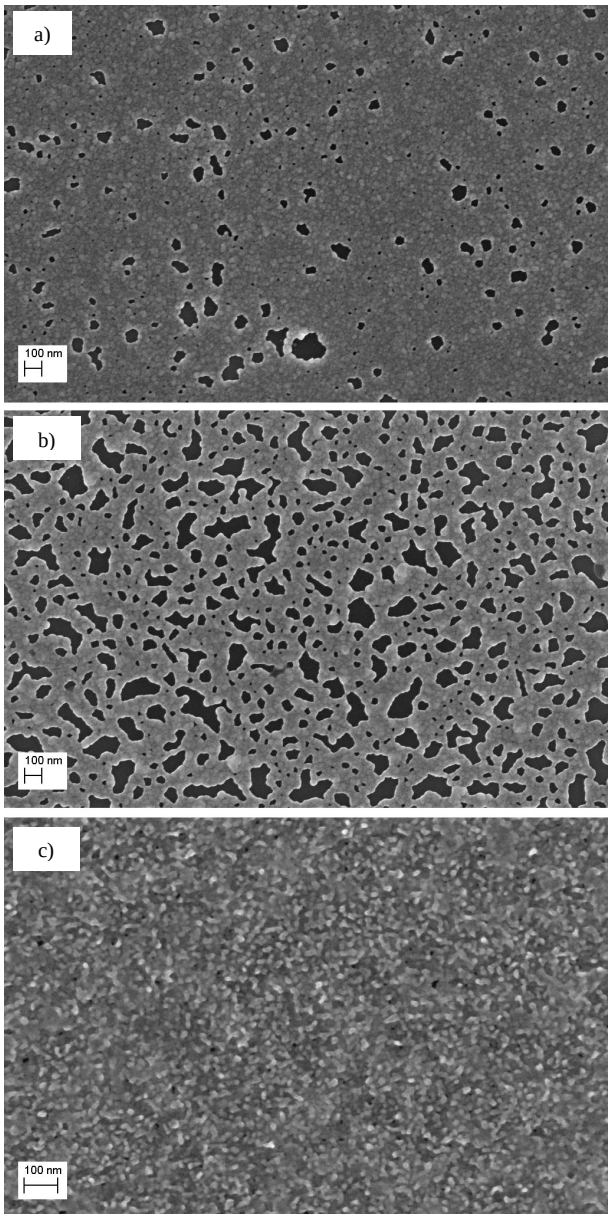

Figure 7. SEM images of the samples reduced in Ar (a), He (b) and N_2 (c) plasma.

spectra of original (Ag) and reduced (Ag-R) silver (sample #2) are compared. The coinciding maxima and minima of Ag and Ag-R prove conversion of semiconductor Ag_xO into metal Ag. Etching in ammonia solution does not affect on samples processed in Ar and He plasma (#1 and #2, respectively), but removes central part of sample #3, processed in N_2 plasma. Only 4 mm wide strip of changed colour was left around sample perimeter after ammonia processing. Fig. 6 shows SEM images of the sample #3 before and after wet etching in the edge area. The observed changing is possible, if the film consists of Ag_2O and Ag. After wet etching Ag_2O is removed, leaving Ag phase on the substrate. SEM images of the central areas of the Ag_xO film processed in Ar (sample #1), He (sample #2) and N_2 (sample #3) plasma are shown in Fig. 7. While Ar and He processed samples demonstrate similar images of silver films with different fragmentation, the image of the sample #3 is more complicate. It can be considered as dark background from Ag_xO at which bright silver inclusions are visible.

The ψ, Δ spectra of reduced Ag_xO for the sample #1 are shown in Fig. 3. They look very similar to spectra of as deposited silver. Reconstruction of sample layers after reduction was done by using optical models shown in Fig. 4b and Fig. 4c. The composite Ag_2O:Ag layer was described by EMA and the model for Ag_2O obtained at oxidation step (Table 1) was used. After that, only thickness and Ag content in layers were changed during matching. In such a way, efficiency of reduction can be estimated by total Ag content in films.

The results of optical measurements are given in Table II. The samples processed in Ar and He can be considered consisting of Ag_2O:Ag layer (thickness h_2) and rough silver layer (thickness h_3), modeled as Ag:air composite. The sample processed in N_2, additionally includes pure Ag_2O layer (thickness h_1) at SiO_2 interface. The total Ag fraction in samples was calculated as average of layer Ag contents according to thickness weight function (fraction of layer thickness in total thickness). Total thickness of all reduced samples is practically the same (Table II) and much less than thickness of Ag_xO film. The thicknesses of as deposited and reduced silver cannot be compared, because they were estimated by quartz microbalance and SE, respectively.

Effect of process parameters on reduction result was studied by monitoring resistivity and Ag content. Fig. 8 demonstrates dependence of these characteristics on process

 ISBN: 978-1-61208-495-4

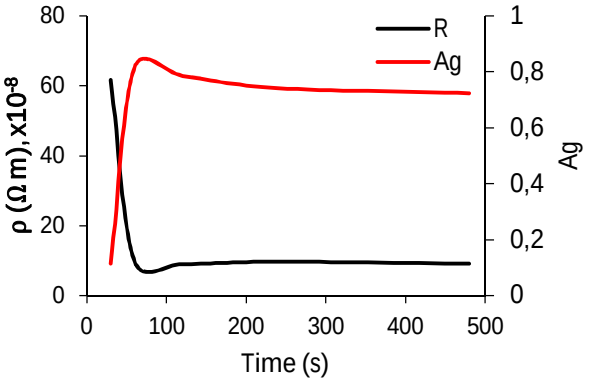

Figure 8. Dependence of resistivity and Ag content on reduction time for film reduced in He plasma.

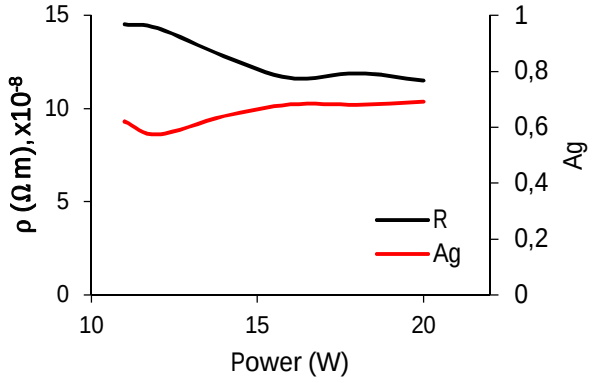

Figure 10. Dependence of resistivity and Ag content on rf power for film reduced in He plasma.

time for PE reactor with He plasma. Fig. 9 and Fig. 10 show variation of resistivity and Ag content with process pressure and rf power, respectively, in RIE reactor with Ar plasma. The fullest reduction happens when processes is done during 60 s at pressure 125 mTor. Mirror like behavior of curves for resistivity and Ag content reflect the fact that Ag inclusions are responsible for electrical conductivity of the samples.

IV. DISCUSSION

The obtained film parameters and SEM images demonstrate synthesis and decomposition of silver oxide during forward reaction of oxidation and reverse reaction of reduction, respectively. Indeed, total transformation of optical and electrical properties of the film after O_2 plasma processing and full restoration of these properties after inert gas plasma treatment (Table II), can be reasonably explained by formation of silver oxide Ag_xO and its conversion into silver, respectively. In this section, we discuss the possible reduction mechanism of silver oxide.

Any sample treated in plasma is bombarded by electrons and ions. The maximum energy of bombarding ions depends on the sample potential. In the PE reactor, the processed sample has potential around 10V relatively plasma. In the RIE reactor, the sample potential is equal to dc self-bias (16 V for sample #1) and depends on process parameters. The beginning of sputtering is defined by threshold energy, which is equal 25 eV and 34 eV for silver sputtering by Ar and He ions,

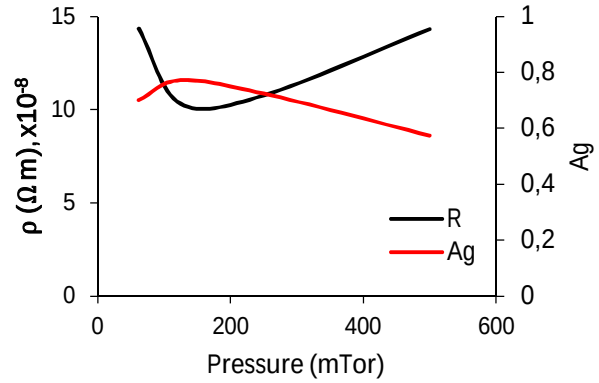

Figure 9. Dependence of resistivity and Ag content on process pressure for film reduced in He plasma.

respectively [11][12]. Therefore, ion energy for He reduction process in the PE reactor is less than threshold sputtering level and sputtering effect cannot be responsible for Ag_xO reduction.

Energy required to break chemical bonds can be delivered in different ways. For example, silver oxide is decomposed on silver and atomic oxygen during low temperature treatment (200 °C) or under UV irradiation. It means that Ag_2O has low bond energy and Ag-O bond can be easily broken. Electron bombardment is often used for breaking chemical bonds. Low energy primary electrons (160 eV) are able to generate secondary electrons, displace oxygen anions and reduce oxides, e.g., TiO_2 [13]. In case of Ag_2O, secondary electron emission is strong enough and starts when primary electron energy exceeds 5 eV. Therefore, reduction of Ag_2O by low energy electrons is also possible and mechanism of plasma reduction is decomposition of Ag_2O on Ag and atomic oxygen under bombardment of electrons ejected from plasma. It means, that reduction rate depends on electron concentration in plasma or degree of its ionization.

At low rf power and low electron energy, most particle collisions in plasma lead to molecule dissociation and excitation, but not to ionization [14]. In monoatomic gases (Ar, He), dissociation is not possible and ionization is more effective than in diatomic gases (N_2). In other words, plasma concentration is higher for Ar and He, than for N_2. In case of sample #3 (N_2 plasma), it explains the lowest reduction rate, demonstrated by the highest resistivity, the lowest Ag fraction and totally different morphology of reduced film in comparison with He and Ar processed samples. Deviation in plasma concentration leads also to different reduction efficiency in Ar and He plasmas. Ionization energy for He and Ar atoms is 25 eV and 16 eV, respectively. Lower ionization energy leads to higher electron concentration in Ar plasma.

Increasing of Ag content with rf power (Fig. 10) is in accordance with dependence of reduction rate on plasma concentration, which is proportional to electrical field strength. However, at rf power higher than 16W, trends in behavior of ρ and Ag content (Fig. 10) are changed. At high power, bias exceeds 25 V, ion energy is above threshold sputtering energy of Ag and sputtering effect becomes significant. It results in preferable silver sputtering from Ag_2O:Ag composite.

 ISBN: 978-1-61208-495-4

Plasma reduction of silver oxide requires only electron impact and can take place in any plasma, e.g., in oxygen one. Silver film oxidized by oxygen plasma is simultaneously exposed to electron irradiation. Electrons facilitate Ag_2O reduction at the same time, when atomic oxygen oxidizes silver. As a result full Ag oxidation does not happen and silver inclusions are observed in Ag_2O obtained in both PE and RIE reactors (Table II).

V. CONCLUSION

Standard parallel plate reactor can be used both for plasma oxidation of silver, and for plasma reduction of silver oxide. In contrast to oxidation, which happens in atomic oxygen ambient, reduction does not require chemically active species and is done in inert gas plasma. Possible reduction mechanism is connected with breaking of Ag-O bonds and generation of secondary electrons. Bond breaking happens due to interaction of silver oxide with electrons and ions of plasma. Rate of plasma reduction is proportional to plasma concentration and can be tuned by plasma gas, rf power and working pressure. Morphology of silver films obtained by processing of Ag_xO in plasma depends on reduction rate and differs for He, Ar and N_2 plasmas.

Sequential silver oxidation and reduction in one reactor may be useful in obtaining of Ag_xO films with controlled silver content.

ACKNOWLEDGMENT

This research was undertaken at the Micronova Nanofabrication Centre, supported by Aalto University.

REFERENCES

[1] E. C. Le Ru and P. G. Etchegoin, Principles of Surface-Enhanced Raman Spectroscopy and Related Plasmonic Effects, Amsterdam: Elsevier, pp. 181-183, 2008.

[2] J. Tominaga, “The application of silver oxide thin films to plasmon photonic devices,” Journal of Physics: Condensed Matter, vol. 15, pp. R1101-R1122, Jun 2003.

[3] G. Saroja, V. Vasu and N. Nagarani, “Optical Studies of Ag_2O Thin Film Prepared by Electron Beam Evaporation Method,” OJMetal, vol. 3, pp. 57-63, 2013.

[4] Gao X.-Y. et al., “Analysis of the dielectric constants of the Ag_2O film by spectroscopic ellipsometry and single-oscillator model,” Physica B, vol. 405, pp. 1922–1926, 2010.

[5] A. C. Nwanya, P. E. Ugwuoke, B. A. Ezekoye, R. U. Osuji, and F. I. Ezema, “Structural and Optical Properties of Chemical Bath Deposited Silver Oxide Thin Films: Role of Deposition Time,” Advances in Materials Science and Engineering, vol. 2013, pp. 1-8, Mar 2013.

[6] W. M. Moor and P. J. Codella, “Oxidation of Silver Films by Atomic Oxygen,” J . Phys. Chem., vol. 92, pp. 4421-4426, Jul 1988.

[7] M. L. Zheludkevich et al., “Oxidation of Silver by Atomic Oxygen,” Oxidation of Metals, vol. 61, pp. 39-48, Feb 2004.

[8] G. Schimo, A. M. Kreuzer, and A. W. Hassel, “Morphology and size effects on the reduction of silver oxide by hydrogen,” physica status solidi (a), vol. 212, pp. 1202–1209, June 2015.

[9] C. C. Tseng, J. H. Hsieh, C. H. Lin, and W. Wu, “Effects of deposition and annealing temperatures on the electrical and optical properties of Ag_2O and Cu_2O–Ag_2O thin films,” J. Vac. Sci. Technol. A, vol. 28, pp. 791-794, 2010.

[10] Philip W. Baumeister, Optical coating technology, Bellingham: SPIE Press, pp. 2-23 - 2-34, 2004.

[11] A. J. van Roosmalen, J. A. G. Baggerman, and S. J. H. Brader, Dry Etching for VLSI, New York: Plemun Press, pp. 65-66, 1991.

[12] E. Hotston, “Threshold energies for sputtering,” Nucl. Fusion, vol. 15, pp. 544-547, 1975.

[13] R. Patel et al., “The defective nature of the TiO_2(110) (1×2) surface,” J. Vac. Sci. Technol. A, vol. 15, pp. 2553-2556, Sep/Oct 1997, doi: 10.1116/1.580769.

[14] M. Lassus and J-P. Founaud, “Modern physics brings semiconductor technology to a turning point,” Microelectronics Reliability, vol. 16 (4), pp. 367-387, 1977.

 ISBN: 978-1-61208-495-4